Enhanced and reduced heat transport in turbulent thermal convection with polymer additives

Article *in* Physical review A, Atomic, molecular, and optical physics · November 2011

DOI: 10.1103/PhysRevE.86.016325

3 authors:

Ping Wei
University of California, Santa Barbara
8 PUBLICATIONS **236** CITATIONS
SEE PROFILE

Rui Ni
Pennsylvania State University
41 PUBLICATIONS **2,648** CITATIONS
SEE PROFILE

Ke-Qing Xia
Southern University of Science and Technology
188 PUBLICATIONS **6,449** CITATIONS
SEE PROFILE

Enhanced and reduced heat transport in turbulent thermal convection with polymer additives

Ping Wei (韦萍), Rui Ni (倪睿), and Ke-Qing Xia (夏克青)
Department of Physics, The Chinese University of Hong Kong, Shatin, Hong Kong, China
(Received 19 November 2010; revised manuscript received 14 June 2012; published 30 July 2012)

We present an experimental study of turbulent Rayleigh-Bénard convection with polymer additives made in two convection cells, one with a smooth top and bottom plates and the other with a rough top and bottom plates. For the cell with smooth plates, a reduction of the measured Nusselt number (Nu) was observed. Furthermore, the amount of Nu reduction increases with increasing polymer concentration (c), reaching ~12% for $c = 120$ ppm and an apparent leveling off thereafter. For the cell with rough plates, however, an enhancement (~4%) of Nu was observed when the polymer concentration is greater than 120 ppm. This increase in Nu is corroborated by an increased large-scale circulation (LSC) velocity in the same cell when polymers are added. In contrast, the LSC velocity in the smooth cell is found to be essentially the same with and without polymers. It is further found that in the smooth cell the rms values of the global Nu, σ_{Nu}, and that of the local temperature, σ_T, both exhibit similar dependence on c as Nu itself. In contrast, σ_{Nu} and σ_T in the rough cell are found to be essentially independent of c.

DOI: 10.1103/PhysRevE.86.016325 PACS number(s): 44.25.+f, 44.20.+b, 47.27.−i, 47.85.lb

I. INTRODUCTION

It is well known that a small amount of polymer additives could reduce the drag significantly in wall-bounded turbulent flows [1]. However, the effect of polymers on heat transport in turbulent flows, such as turbulent thermal convection, is much less known and has been drawing attention only very recently. The Rayleigh-Bénard (RB) system has served well as a paradigm for studying the general turbulent thermal convection phenomenon [2,3]. When the geometry and aspect ratio of the convection cell are fixed, the system is characterized by two control parameters: the Rayleigh number ($\mathrm{Ra} = \alpha g H^3 \Delta T/\nu\kappa$) and the Prandtl number ($\mathrm{Pr} = \nu/\kappa$), where g is the gravitational acceleration; α, ν, and κ, respectively, are the volume expansion coefficient, the kinematic viscosity, and the thermal diffusivity of the convecting fluid; and ΔT is the temperature difference across the fluid layer of height H. Recently, a heat transport experiment was conducted in an RB convection cell with polymers and a monotonic decrease of the Nusselt number (Nu, the ratio of actual heat flux over that if there were only conduction) with increasing polymer concentration was found [4]. On the other hand, direct numerical simulation (DNS) studies have shown that it is possible to achieve an increase in Nu in bulk turbulent thermal convection, which has been demonstrated in RB convection by replacing the top and bottom solid walls with periodic boundary conditions [5] and in Rayleigh-Taylor turbulence that naturally has not boundary layers [6]. The realization of bulk (or homogeneous) turbulent RB convection with periodic boundary conditions was first realized in an earlier DNS study [7]. If a small amount of polymer additives can indeed enhance heat transport, it would be important for many practical applications involving heat management, in addition to its obvious importance in the fundamental studies of turbulent flows. Theoretically, the thermal and kinetic dissipation rates in turbulent thermal convection may be decomposed into contributions from the bulk and the boundary layers (BLs) and which of these plays a dominant role depends on the range of Ra and Pr considered [8]. In the above DNS studies, the enhanced heat transfer is thought to result from the stretching of polymers in the turbulent bulk flow [5,6]. In the experimental study of Ref. [4], the reduced Nu is thought to result from the increased drag in the boundary layer region due to the polymer additives. While it is not easy to remove the solid walls in an experiment, in a recent study it has been found that the use of top and bottom plates with rough surfaces can result in Nu behavior that is consistent with a more bulk-dominant convection regime [9]. This result inspires the present work, which is a comparative experimental study of turbulent heat transport with polymer additives in two convection cells: one with smooth top and bottom plates and one with rough top and bottom plates.

The remainder of this paper is organized as follows. In Sec. II A, we describe the convection cells used in the experiments and experimental conditions and parameters. Section II B presents the viscosity measurement of the polymer solutions. In Sec. II C the calibration of the temperature probes and method for local temperature measurements are discussed. Section II D describes how the large-scale circulation (LSC) velocity U and the corresponding Reynolds number Re are determined from local temperature oscillations and a comparison of the measured Re with those from previous studies. The experimental results are presented in Sec. III, which is divided into three parts. Section III A presents measured results of the time-averaged Nusselt number from both the smooth and the rough cells, with and without polymer additives. Section III B discusses the time-dependent behavior of the Nu and the statistical properties of local temperature fluctuations. In Sec. III C we show the effect of polymer additives on the measured velocity and the Reynolds number for both the smooth and the rough cells. In Sec. IV, we discuss and analyze the results and provide some plausible explanations for the observed heat transport reduction and enhancement. We summarize our findings and conclude in Sec. V.

II. EXPERIMENTAL SETUP AND METHODS

A. The convection cell and experimental parameters

In the experiments, two convection cells have been used that have top and bottom plates with smooth and rough surfaces, respectively. They are otherwise identical and are referred as

"smooth" and "rough" cells hereafter. The construction of both cells are similar to the smooth and rough cells that were used in previous studies and were described in detail in Refs. [10,11] respectively. The main difference is that, in the present case, the top and bottom plates of both cells are made of aluminum and their surfaces are coated with a thin layer of Teflon to prevent the adsorption of polymers on the metal surface. Schematics of the two cells together with the probe configuration for local temperature measurements are shown in Fig. 1. Briefly, these are upright cylinders with aluminum plates at the top and bottom and Plexiglas tube as the sidewall. The rough surface consists of pyramids directly machined on a single piece of aluminum and arranged in a latticelike structure. The height of the pyramids is $k = 8$ mm. The diameter of the smooth (rough) cell is 19.4 (19.2) cm and their height is 20.0 cm (for the rough cell this was measured from the valley of the pyramids). The heating of the cell is provided by a resistive heater attached to the back of the bottom plate and the cooling is provided by a refrigerated circulator passing temperature-controlled water through a chamber fitted to the top plate. Three layers of Styrofoam are wrapped outside the sidewall. To prevent heat leakage, a copper basin is placed under the cell (with three layers of plywood in between) and is regulated at a temperature equal to that of the bottom plate. The apparatus is placed in a thermostat box, which is at a temperature equal to that of the bulk fluid in the cell. The temperature difference ΔT across the cell was measured by thermistors imbedded inside the plates, four in the top plate and five in the bottom one. In previous studies of turbulent convection using similar rough cells made with copper or brass [11,12], it has been found that many of the qualitative features of the temperature and velocity fields are similar as those found in the smooth surface cells, such as the scaling of the velocity boundary layer thickness and the shape the temperature histograms. It was found that the most significant feature in the rough surface cells is the enhanced emission of thermal plumes from the tip of the pyramids, which is largely responsible for the enhanced heat transport in this cell.

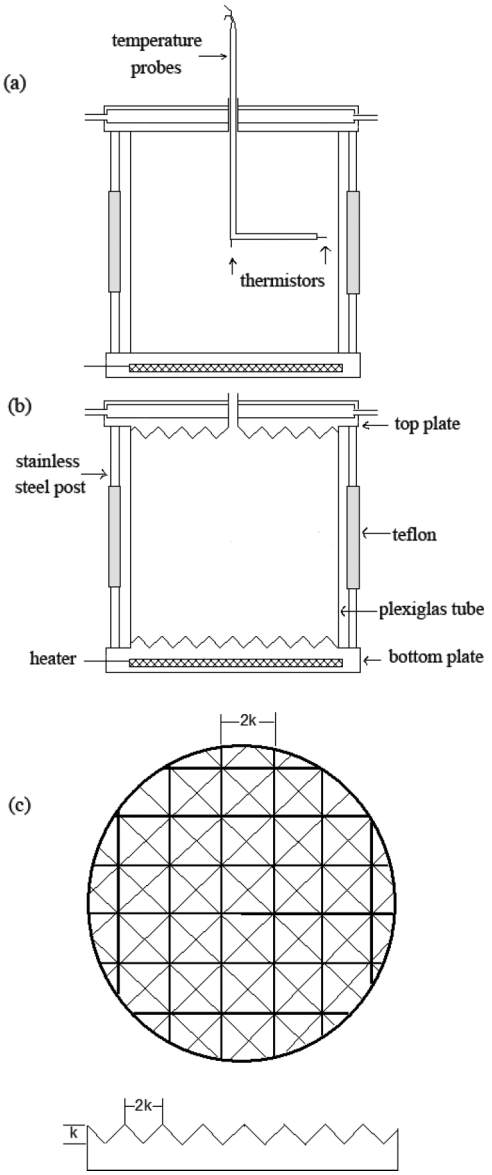

FIG. 1. Schematic diagram of the convection cells. (a) The smooth cell. Also shown are thermistor probes for measuring local temperatures at cell center and near sidewall. (b) The rough cell. (c) Sketch of the geometry of the roughness elements: square pyramids with height k and base width $2k$ (here $k = 8$ mm) (sketch adopted from Ref. [11]).

In both the smooth and the rough cells, two types of parameter scans were made in the experiment. For the smooth cell, measurements of Nu and the local properties were made at approximately the same Ra $\approx 8.1 \times 10^9$ for various polymer concentrations (the concentration scan). In addition, measurements were made with varying Ra for two concentrations $c = 0$ and 120 ppm, respectively (the Ra scan). For the rough cell, the concentration scan was made at Ra $\approx 5.4 \times 10^9$ and the Ra scans were conducted for four concentrations ($c = 0$, 120, 150, and 180 ppm). All measurements were made at constant input heat flux at the bottom plate with the center temperature of fluid maintained at 40.0 °C, corresponding to Pr = 4.34 for the case of pure fluid.

B. Measurement of the polymer solution viscosity

To measure the viscosity of polymer solution, we use a glass capillary viscometer similar to the Ostwald viscometer [13]. We place the viscometer vertically in a water bath where the temperature is controlled at 40 °C, which is the same as the temperature of the bulk fluid in the convection cell. In the experiment, the diameter of capillary tube used is 0.4 mm. We inject the fluid from the arm of viscometer with large tube until the big bulb is filled and wait for the fluid in the bulb reaching thermal equilibrium. Liquid is drawn into the upper two bulbs by suction and then allowed to flow down through the capillary into the lower bulb. The time taken for the level of the liquid to pass between these marks is proportional to the kinematic viscosity. The viscometer was calibrated using literature value of the viscosity of water at 40 °C.

The polymer used was PEO (polyethylene oxide) with a nominal molecular weight of 4×10^6 g/mol. The effect of polymer additives on most physical properties of water is generally believed to be negligible in the low concentration range such as in our experiment [14], except the viscosity. It is known that polymer solutions are non-Newtonian fluids,

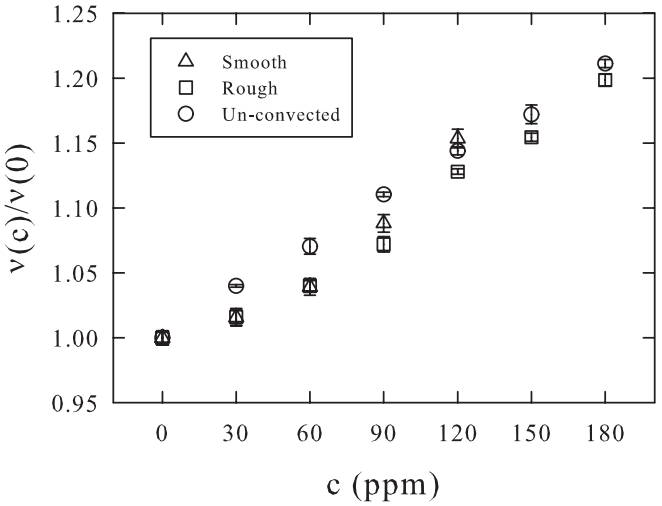

FIG. 2. Measured kinematic viscosity of polymer solutions normalized by that of water as a function of polymer concentration at 40.0 °C.

which means its viscosity is shear-rate dependent. However, a previous study using PEO of the same nominal molecular weight as in the present work has found no shear-thinning behavior for concentrations below 200 ppm [15]. Figure 2 plots the measured viscosity of polymer solutions normalized by that of pure water as a function of polymer concentration c (in weight ppm, hereafter simply ppm). Three sets of data are shown in the figure: (1) "unconvected" polymer solutions, i.e., viscosity was measured before the solution being injected into the convection cell; (2) solutions drawn from the smooth cell after Nu measurement was done in that cell; and (3) solutions drawn from the rough cell after Nu measurement in that cell. The "convected" solutions have been in the smooth (rough) cells for a duration from a few days to several weeks, depending on the concentration. It is seen from the figure that the solution viscosity increases with polymer concentration monotonically, but, in general, the viscosity of the convected solutions are smaller than that of the unconvected ones. This may be an indication that some polymers have been adsorbed on the walls of the convection cell, resulting in a concentration smaller than the nominal value. Overall, the viscosities of the "convected" and "unconvected" solutions are very close to each other and their differences are a few percentages at most. As the solution viscosity depends on such things as the concentration of the polymer, its molecular weight and conformations, this result suggests that, after many weeks under turbulent thermal convective flow, no significant changes of polymer properties have occurred. Hereafter, all concentrations refer to the nominal value and the measured $\nu(c)$ of the convected fluid were used in the calculation of Ra for the corresponding solutions.

C. Local temperature measurement

In the present work, we use two kinds of thermistors to measure the local temperature. In the plate, embedded expoxy-encapsulated round metallic probes with diameter 2 mm (44031, OMEGA Engineering, Inc.) are used. These probes have an accuracy of ±0.01 °C. In the fluid, two high-sensitivity metal oxides NTC thermistors with diameter 0.3 mm and accuracy ±0.1 °C (AB6E3-B07, GE Measurement and control Inc.) are used to measure the temperature of the convecting fluid. These smaller probes have higher sensitivity but their accuracy is lower than those of the larger probes. In the present work, they are used to measure local temperature fluctuations inside the cell and only the difference from the mean, not the absolute, value of the measured temperature is used. As shown in Fig. 1(a), the small thermistors are fixed on an L-shaped stainless steel rod and are used to measure the center and sidewall (about 1 cm away from the wall and at midheight) temperatures, respectively.

A $6\frac{1}{2}$ digit multimeter (Keithley Model 2700) is used to measure the resistance of the themistors. The resistance data is taken at a sampling rate of about 1 Hz. The measured resistance of each thermistor can be well described by the equation: $1/T = a + b(\log R) + c(\log R)^2 + d(\log R)^3$ [16], where T is the absolute temperature, R is the measured resistance of the thermistor at the corresponding temperature, and the coefficients a, b, c, and d are determined from calibrations. For each Ra, we usually wait for 8 h until the system has reached the steady state, and the typical duration for temperature recording is about 8 h, which is sufficient for obtaining second-order statistical quantities such as the rms and the correlation functions.

D. Velocity measurement

It is well known that there exists a coherent low-frequency oscillation in turbulent thermal convection, which can be detected from both temperature and velocity measurements [17–22]. To measure the velocity of the LSC, we analyze the autocorrelation function $C(\tau) = \langle \delta T(t)\delta T(t+\tau)\rangle / \langle (\delta T)^2 \rangle$, where $\delta T(t) = T(t) - \langle T \rangle$ and $T(t)$ is the local temperature measured by the thermistor placed near the sidewall (at midheight) of the cells and the bracket $\langle \cdots \rangle$ denotes a time average. Figures 3(a) and 3(b) show examples of autocorrelation functions measured in the smooth and the rough cells, respectively, and for cases without polymers (red solid line) and with polymers (blue dashed line). It is seen that the measured $C(\tau)$s all exhibit well-defined oscillations. (Note that in Fig. 3(b) the oscillation period for $c = 180$ is smaller than in the $c = 0$ case, suggesting a faster flow. This will be discussed in detail in Sec. III C.) We take the position of the second peak as the turnover time t_T of the LSC and define $U = 4H/t_T$ as the typical velocity of convective flow. We also calculate the Reynolds number, $\mathrm{Re} = UH/\nu(c)$, based on the velocity of LSC and the viscosity of fluid. In the range of Ra in the present work, the turnover time spans from 30 to 120 s and the finite sampling rate introduces a systematic error of ∼3% in the measured turnover time.

As a check for our measurement, we compare in Fig. 4 the measured Re (without polymers) from the present work with results from some previous studies. In the figure, the circles represent measurements made in the present Teflon-coated smooth-surface aluminum plate cell, the triangles represent those made in a gold-coated smooth surface copper plate cell [23], the squares are from the present Teflon-coated rough-surface aluminum plate cell, inverted triangles are from gold-coated rough-surface copper plate cell [24], and crosses are

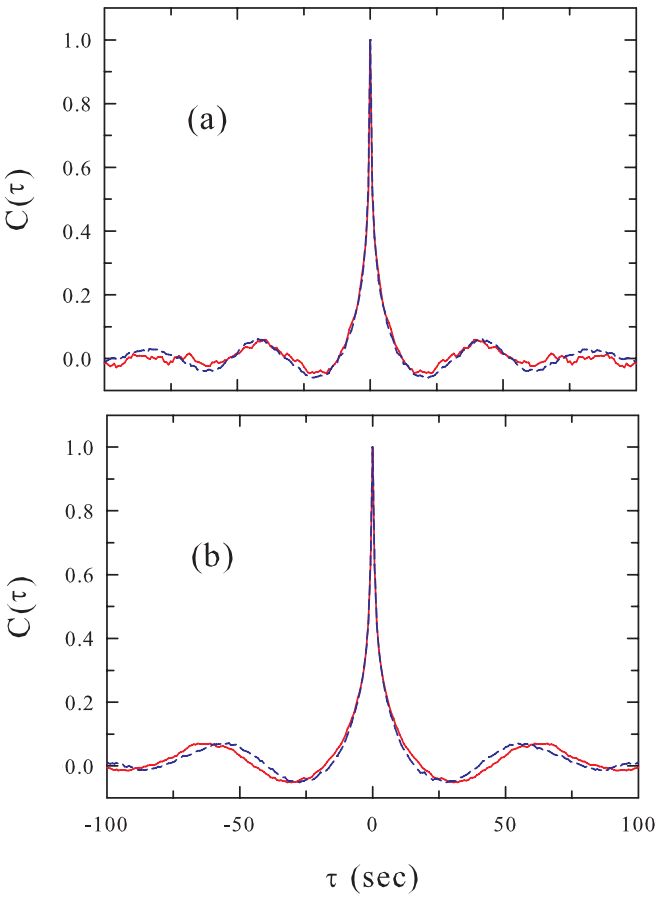

FIG. 3. (Color online) Autocorrelation functions of temperature fluctuations measured near sidewall: (a) in the smooth cell at Ra = 8×10^9, solid (red) line, 0 ppm; dashed (blue) line, 120 ppm; (b) in the rough cell at Ra = 2×10^9, solid (red) line, 0 ppm; dashed (blue) line, 180 ppm.

from anodized rough-surface aluminum plate cell [24]. It is seen that the present results show excellent agreement with those from previous studies for the same type of cell (smooth or rough), irrespective of the surface coatings and plate materials used. In the figure the solid lines represent power law fits to the data from the present measurements in the smooth and rough cells, respectively. The fitting results are given in the figure caption.

III. RESULTS

A. The Nusselt number measurement

We show in Fig. 5 measured Nu in the smooth and rough cells *without* polymers. For comparison, we also plot results measured in previous studies in both rough and smooth cells. In the figure, the squares and circles are from the present study, measured in the rough and smooth cells, respectively; the triangles were measured in a rough-surface gold-coated copper cell [24]; the inverted-triangles were measured in a smooth-surface gold-coated copper cell [25] (all data in the figure are for the same Pr = 4.3). The figure shows that Nu measured in the present study using Teflon-coated aluminum plates are in excellent agreement with those measured in gold-coated copper plates for both smooth and rough cases

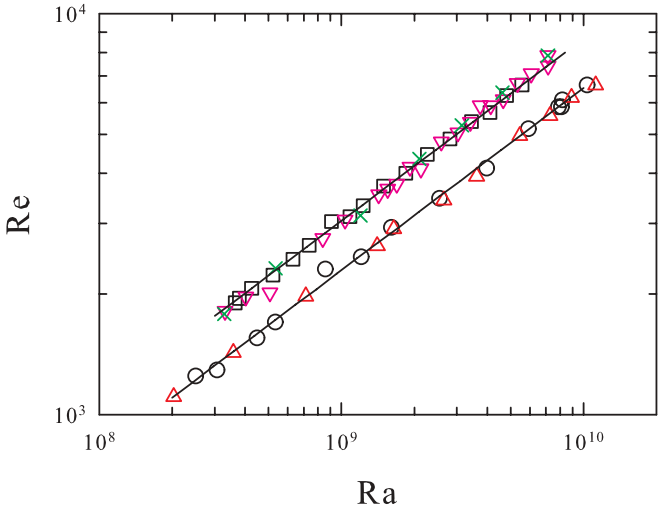

FIG. 4. (Color online) The Reynolds number measured in pure fluid *without* polymers in various convection cells of different boundary conditions, surface treatments, and plate materials. (Circles) Teflon-coated smooth-surface aluminum plate cell (present work); (triangles) gold-coated smooth-surface copper plate cell (Ref. [23]); (squares) Teflon-coated rough-surface aluminum plate cell (present work); (inverted triangles) gold-coated rough-surface copper cell (Ref. [24]); and (crosses) anodized rough-surface aluminum cell (Ref. [24].) The solid lines represent power-law fits to the respective data from the present work. (Lower solid line) $\mathrm{Re} = (0.19 \pm 0.03)\mathrm{Ra}^{0.45\pm0.01}$; (upper solid line) $\mathrm{Re} = (0.25 \pm 0.02)\mathrm{Ra}^{0.45\pm0.01}$.

and that Nu in the rough cell is larger than that of the smooth one in both its magnitude and its scaling exponent with Ra. In the figure, the solid lines are power-law fits to the respective data from present study: $\mathrm{Nu} = 0.1772\mathrm{Ra}^{0.28}$ (smooth) and $\mathrm{Nu} = 0.065\mathrm{Ra}^{0.36}$ (rough). Figure 5 thus shows that our present smooth and rough cells made of aluminum plates with Teflon coating produce the same Nu-Ra relationships as those found respectively in smooth and rough cells made of copper plates.

We now present results *with* polymers. As the measurements are made under the condition of constant heat flux at bottom plate, when polymers are added to the fluid the temperature difference across the cell, ΔT, will change, resulting in a change of Ra. This means that for measurements under the same heat flux but with different polymer concentrations, the corresponding Ra will vary slightly (about a few percentages). When presenting the data, we will use the value of Ra for the pure fluid ($c = 0$) case as the nominal value. When normalizing the measured Nu(c) by its pure fluid value, we use Nu(0) corresponding to the actual Ra of that data point as obtained from the fittings to the pure fluid Nu shown in Fig. 5. In Fig. 6(a), we show measured Nu from the smooth cell in a compensated plot, where data measured at the nominal Ra ($\approx 8.1 \times 10^9$) but with varying polymer concentration c and data with fixed concentration ($c = 120$ ppm) but varying Ra are plotted. In Fig. 6(b) we show Nu(c) normalized by its corresponding value in pure water for the same Ra, with a nominal value of $\mathrm{Ra} = 8.1 \times 10^9$. Figure 6 shows that the Nu decreases monotonically with increasing polymer concentration up to $c = 120$ ppm and then appears to level off afterwards and that for a fixed c the Ra

dependency of Nu is similar to the $c = 0$ case. The trend of Nu decreases with increasing polymer concentration is similar to the findings in Ref. [4]. However, the saturation of Nu reduction for $c \geqslant 120$ ppm has not been observed previously (in Ref. [4], the highest c reached was 120 ppm).

In contrast to the results found in the smooth cell, the measured Nu from the rough cell show quite different behavior. As shown in Fig. 7, the measured Nu first decreases slightly with increasing polymer concentration but then increases above the value for pure water. To confirm the enhanced heat transport, we made the Ra scan for three concentrations: c =120, 150, and 180 ppm. The results all show clearly that the measured Nu is higher than the corresponding values for pure water. The heat transfer enhancement, for polymer concentrations larger than 120, although only a few percentages, is quite significant. It provides a direct evidence that it is possible to enhance heat transfer in turbulent convective flows by adding polymers. To our knowledge, this is the first time such enhancement has been found experimentally. Note that measurements were also made at two additional concentrations ($c = 210$ and 240 ppm), and the Nu showed a decrease relative to that of the pure fluid. As the additional polymers to achieve these concentrations were added a few weeks after the initial measurements were finished, there might be polymer degradation or adsorption on the walls during this period, resulting a lower polymer concentration than the nominal value. Because of this, these two points are not shown in Fig. 7 to avoid creating confusion.

B. Fluctuations of Nu and the local temperature

To shed some light on the above results, we examine the fluctuations of the global Nu. The instantaneous Nu(t) is determined from the instantaneous $\Delta T(t) = T_b(t) - T_t(t)$, where $T_b(t)$ is the instantaneous (spatially averaged) temperature of the four (five) thermistors imbedded in the bottom plate of the smooth (rough) cell and $T_t(t)$ is the instantaneous average temperature of the four thermistors imbedded in the top plate of the smooth and rough cells. Figure 8(a) plots sample time traces of Nu(t) measured in the smooth cell in a period of over 4 h (Ra $= 5 \times 10^9$). The polymer concentrations are, from top to bottom, 0, 30, 60, 90, and 120 ppm. It is seen that on this scale of resolution the measured Nu shows small fluctuations. But, in addition to the reduced magnitude of Nu with increasing polymer concentration, as we already see in the previous section, the amplitude of fluctuations also seems to decrease with increasing c. This can be seen more clearly in Fig. 8(b), where it is seen that the standard deviation of the fluctuating Nu decreases gradually from 0.4 for $c = 0$ to below 0.25 for $c \geqslant 120$ ppm and then levels off for c above 120 ppm, which corresponds to the relative fluctuation $\sigma_{\rm Nu}$/Nu varying from ~0.35% to ~0.2%. Figure 8(c) plots normalized $\sigma_{\rm Nu}(c)/\sigma_{\rm Nu}(0)$ vs c and it is seen that the rms fluctuation is reduced by about 40% for $c \geqslant 120$ ppm as compared to its

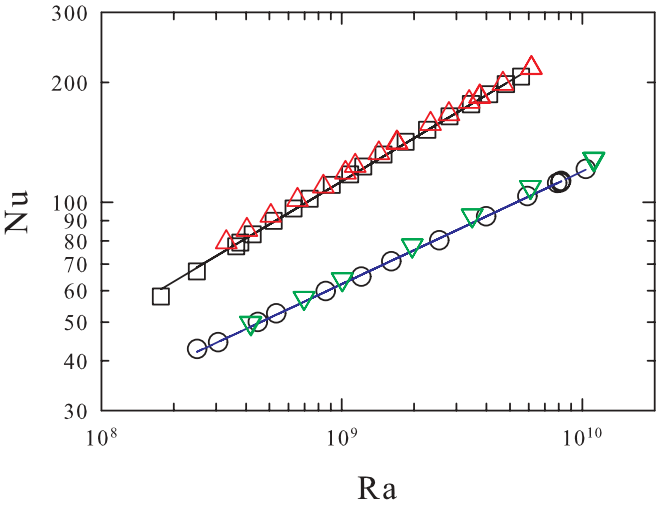

FIG. 5. (Color online) Nu measured in pure fluid *without* polymers. (Squares) Teflon-coated aluminum rough-surface cell (present work); (triangles) gold-coated copper rough-surface cell (Ref. [24]); (circles) Teflon-coated aluminum smooth-surface cell (present work); (inverted triangles) gold-coated copper smooth-surface cell (Ref. [25]). The solid lines represent power-law fits to the respective data from the present work. (Lower solid line) $N_u = 0.1772\ \mathrm{Ra}^{0.28}$; (uppper solid line) $N_u = 0.065\ \mathrm{Ra}^{0.36}$.

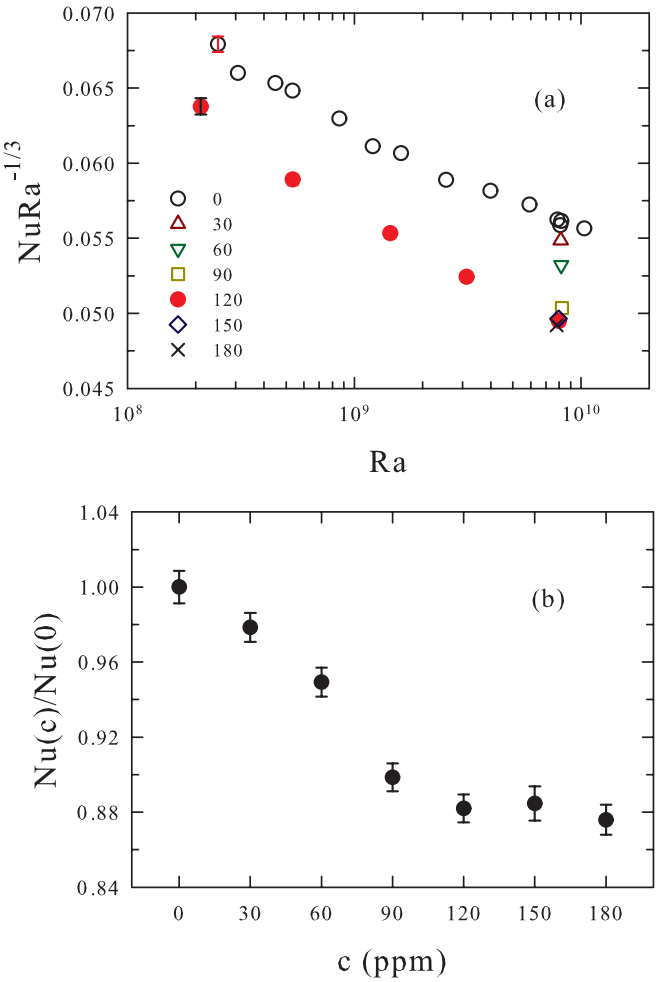

FIG. 6. (Color online) Smooth cell results. (a) Compensated Nu as a function of Ra for polymer concentration $c = 120$ ppm (solid circles). Also shown are compensated Nu measured with c varying from 30 to 180 ppm at approximately the same Ra $\approx 8.1 \times 10^9$. The open circles represent pure fluid result. (b) Nu normalized by pure fluid value versus polymer concentration c. The nominal value of Ra is 8.1×10^9 for all data points.

pure liquid value. (As with the case of normalized Nu, the values of Ra shift slightly for data with different c. So the value of $\sigma_{\mathrm{Nu}}(0)$ used to normalize each $\sigma_{\mathrm{Nu}}(c)$ is obtained from the fitted $\sigma_{\mathrm{Nu}}(c)$ vs Ra relation for the actual value of Ra for each c and is not exactly the same as $\sigma_{\mathrm{Nu}}(0)$ for the nominal Ra. This is why some data points in Fig. 8(c) look higher than the $c = 0$ value. The same situation also applies for Fig. 9(c).) Interestingly, the apparent leveling off of σ_{Nu} for $c \geqslant 120$ ppm similarly mirrors the behavior of Nu itself [see Fig. 6(b)]. In contrast, as shown in Fig. 9(a), Nu fluctuation in the rough cell is greatly enhanced (for clarity, only $c = 0$ and 120 ppm are shown; note also that the scale is the same as in Fig. 8(a)). As shown in Fig. 9(b), the enhanced fluctuations of Nu occur for all concentrations. Moreover, rather than decreasing with increasing polymer concentration, $\sigma_{\mathrm{Nu}}(c)$ in the rough cell remains essentially the same for all concentrations, including the $c = 0$ case. Figure 9(c) plots the normalized $\sigma_{\mathrm{Nu}}(c)/\sigma_{\mathrm{Nu}}(0)$ vs c. It is seen that, in comparison to the $c = 0$ value, the standard deviation of Nu for fluids with polymers decreases

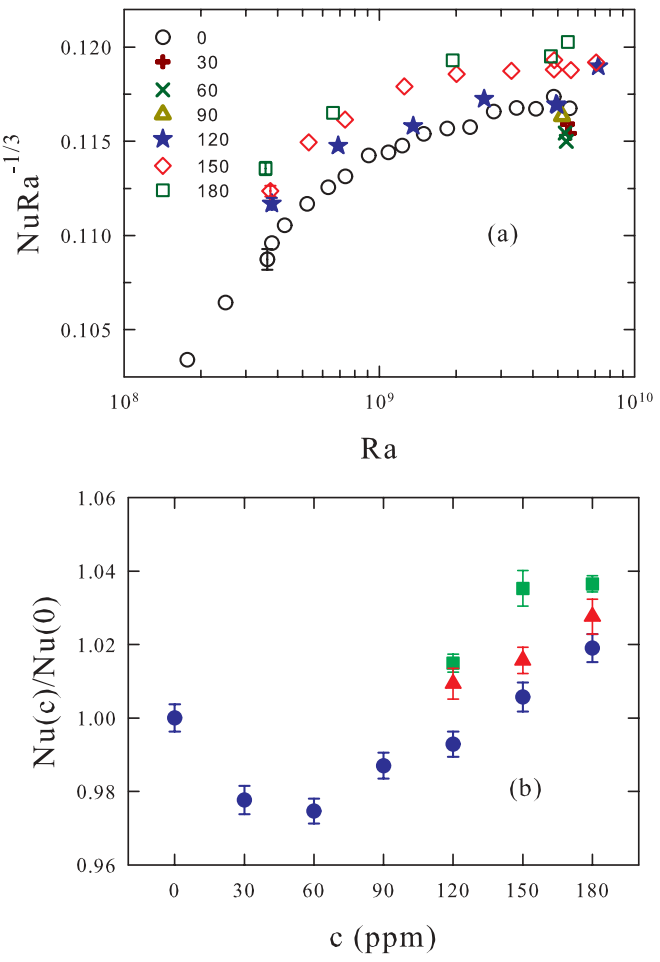

FIG. 7. (Color online) Rough cell results. (a) Compensated Nu as a function of Ra for polymer concentrations $c = 120$ ppm (stars), 150 ppm (open diamonds), and 180 ppm (open squares). Also shown are compensated Nu measured with c varying from 30 to 180 ppm at approximately the same Ra $\approx 5.4 \times 10^9$. The open circles represent pure fluid result. (b) Nu normalized by pure fluid value versus polymer concentration c for several values of Ra: 5.4×10^9 (circles), 1.3×10^9 (squares), and 3.7×10^8 (triangles).

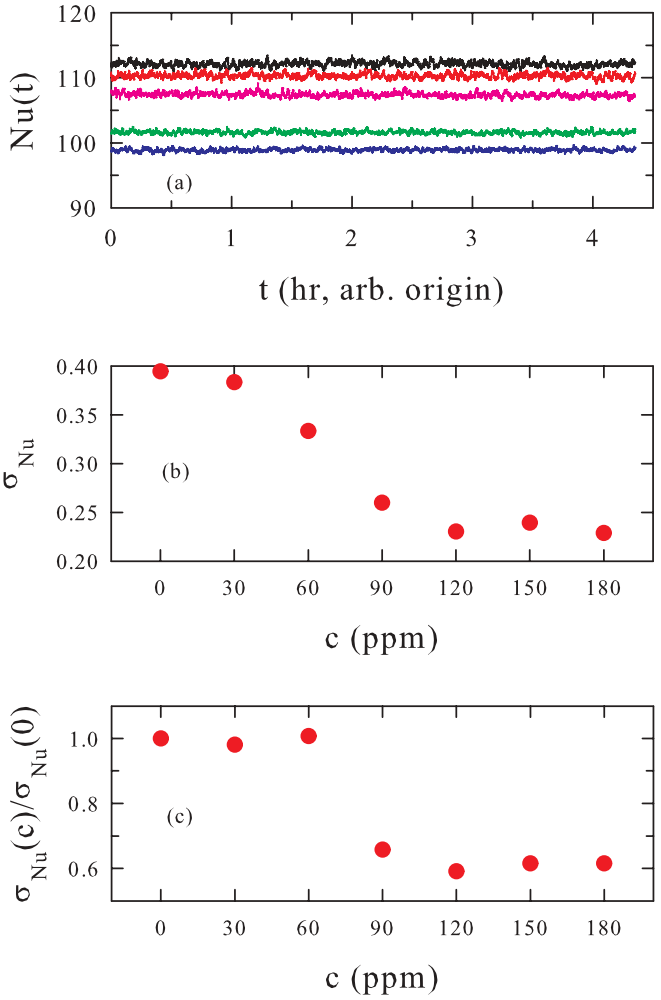

FIG. 8. (Color online) Results from the smooth cell (nominal Ra $= 8 \times 10^9$). (a) Sample time series of Nu(t) measured at various polymer concentrations, from top to bottom, $c = 0$, 30, 60, 90, and 120 ppm. (b) The standard deviation of Nu(t) as a function of c. (c) The standard deviation $\sigma_{\mathrm{Nu}}(c)$ normalized by its pure fluid value versus polymer concentration c.

at most a few percentages, which is in sharp contrast with the nearly 40% drop of $\sigma_{\mathrm{Nu}}(c)$ in the smooth cell. (For $c = 180$, $\sigma_{\mathrm{Nu}}(c)$ is seen to be slightly higher than the $\sigma_{\mathrm{Nu}}(0)$ value. We note that the averaging time for this concentration was significantly shorter than most of the other samples, and, being a second-order quantity, the standard deviations usually require long averaging times to be measured accurately.)

The above observed fluctuating properties of the global Nu are corroborated by the properties of the local temperature fluctuations. We examine the results measured at the cell center first. Figure 10(a) plots the rms value σ_T of the local temperature measured in the smooth cell, normalized by the temperature difference ΔT across the cell, versus polymer concentration. It is seen that the trend of local temperature fluctuation at cell center clearly follows the fluctuation of the global Nu. Figure 10(b) shows $\sigma_T/\Delta T$ measured in the rough cell for three values of Ra and various polymer concentrations. Similarly to σ_{Nu} for the rough cell and in contrast to the smooth cell case, the local temperature fluctuations do not

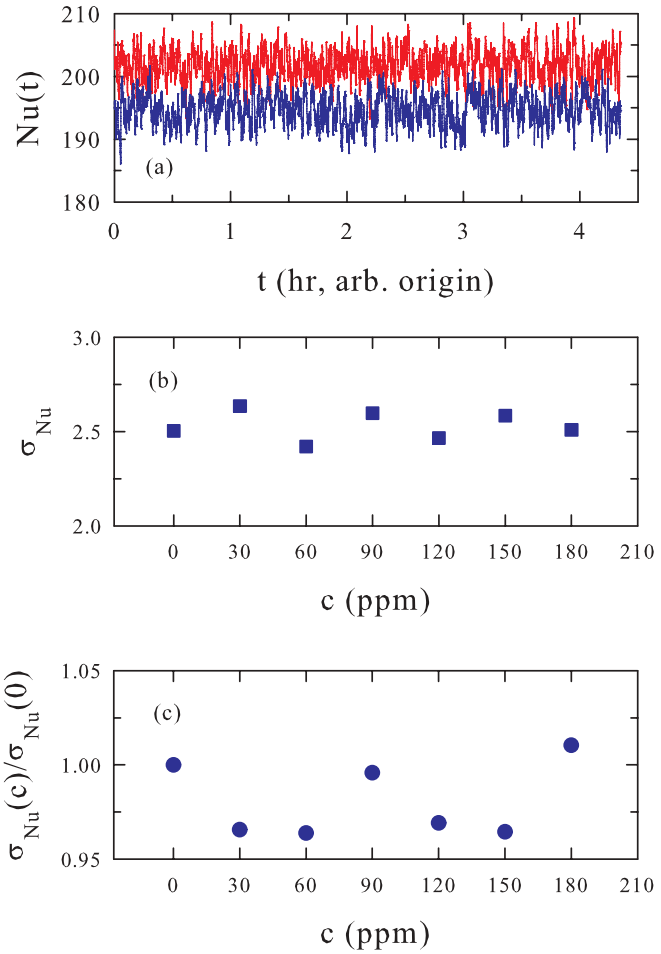

FIG. 9. (Color online) Results from the rough cell (Ra $= 5.4 \times 10^9$). (a) Sample time series of Nu(t) for $c = 0$ (upper trace) and $c = 120$ ppm (lower trace) (b) The standard deviation of Nu(t) as a function of c. (c) The standard deviation $\sigma_{\rm Nu}(c)$ normalized by its pure fluid value versus polymer concentration c.

show sensitive dependence on the polymer concentration. For the sidewall, as shown in Fig. 11, the trend is similar to that in the center, i.e., no sensitive dependence on c in the rough cell and the magnitude of temperature fluctuations in the rough cell is much larger than that in the smooth cell. One difference is that in the smooth cell, the concentration dependence of $\sigma_T/\Delta T$ is more scattered and does not show a clear trend as in the cell center.

We next look at the Ra-dependent properties of the local temperature fluctuations, which are shown in Figs. 12 and 13, respectively. In general, the normalized local temperature fluctuations may be written as a power law of Ra, i.e., $\sigma_T/\Delta T = A{\rm Ra}^{\beta}$. In the main part of Fig. 12 we show a log-log plot of σ_T(center)$/\Delta T$ vs Ra measured from both the smooth (circles) and rough (squares, triangles, and diamonds) cells and for various polymer concentrations. Although there is some scatter in the data, they all can be fitted to power laws with the results shown in Table I. In the figure, for clarity, only fittings for the $c = 0$ cases are shown (solid lines). In the inset of the figure, compensated plots of $\sigma_T/\Delta T$ are shown. These results again show that fluctuations in the rough cell are greatly enhanced compared to those in the smooth cell. As

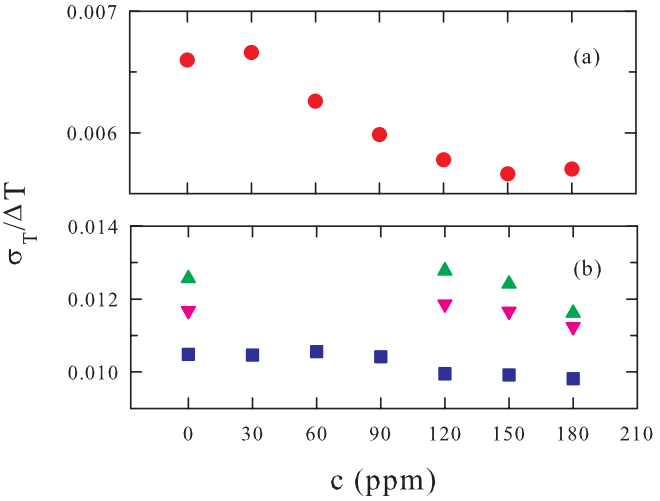

FIG. 10. (Color online) Measured $\sigma_T/\Delta T$ at the cell center as a function of c: (a) in the smooth cell (Ra $= 8 \times 10^9$); (b) in the rough cell. (Squares) Ra $= 5.4 \times 10^9$, (upward-pointing triangles) 1.3×10^9, and (downward-pointing triangles) 3.7×10^8.

shown in Fig. 10, polymer additives in both the smooth and rough cells tend to suppress the local temperature fluctuations. But the effect is much stronger in the smooth cell and less so in the rough cell. A notable feature is that, similarly to $\sigma_{\rm Nu}$, σ_T in the smooth cell exhibits a similar trend to that of Nu itself, i.e., all three quantities have similar concentration dependence. Note also that the effect of polymer additives on σ_T in both cells is only secondary to the difference between those caused by the surface of the cell. We remark that the scaling exponent β is difficulty to determine accurately in experiments. Part of the reason is that the rms is a second-order quantity and the absolute value of this exponent is also very small. This is why the value of β reported in the literature varies over a rather wide range from -0.05 to -0.19 [26]. It is seen from Table I, for the smooth cell, that the scaling exponent of $\sigma_T/\Delta T$ is consistent with results from previous studies. The exponent

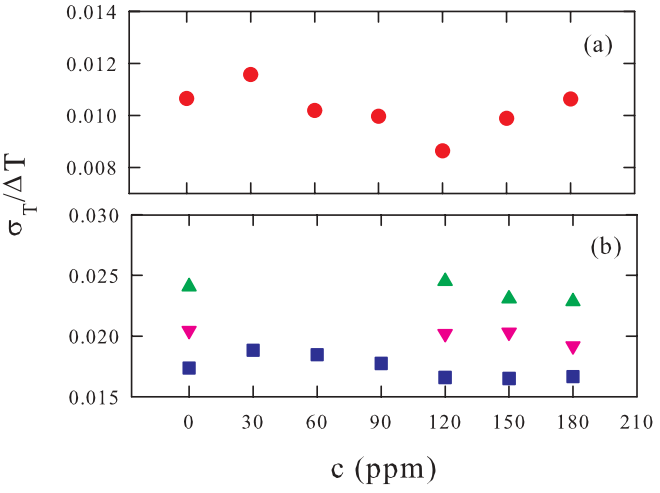

FIG. 11. (Color online) Measured $\sigma_T/\Delta T$ near the sidewall as a function of c: (a) in the smooth cell (Ra $= 8 \times 10^9$); (b) in the rough cell. (Squares) Ra $= 5.4 \times 10^9$, (upward-pointing triangles) 1.3×10^9, and (down-pointing triangles) 3.7×10^8.

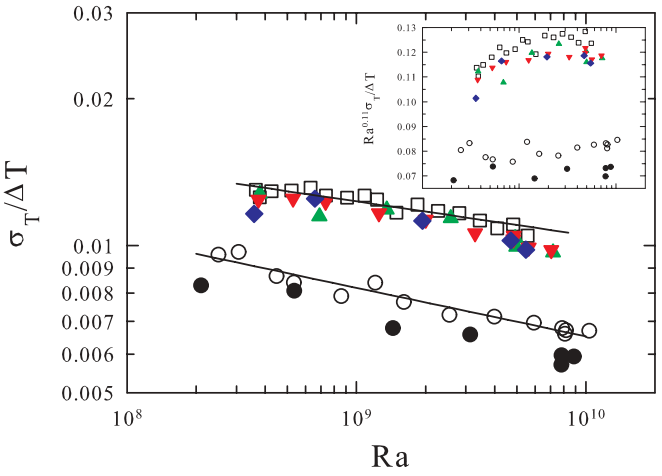

FIG. 12. (Color online) $\sigma_T/\Delta T$ measured at the cell center as a function of Ra: (open circles) smooth cell, $c = 0$; (solid circles) smooth cell, $c = 120$; (open squares) rough cell, $c = 0$; (solid triangles) rough cell, $c = 120$; (solid inverted triangles) rough cell, $c = 150$; (solid diamonds) rough cell, $c = 180$. The solid lines represent power-law fits to the $c = 0$ case in the smooth and rough cells, respectively. (Inset) Compensated plots of the same data as in the main figure.

obtained in the rough cell, however, is somewhat smaller than those found in the smooth cells.

As shown in Fig. 13, the results measured near the sidewall are qualitatively similar to those obtained in the cell center, i.e., the magnitude of local temperature fluctuations are greatly enhanced in the rough cell compared to that in the smooth case. The results can all be well described by power laws with the fitting results also listed in Table I. For the smooth cell, there are very few results of β (either experimental or numerical) that exist in the literature for $\sigma_T/\Delta T$ measured

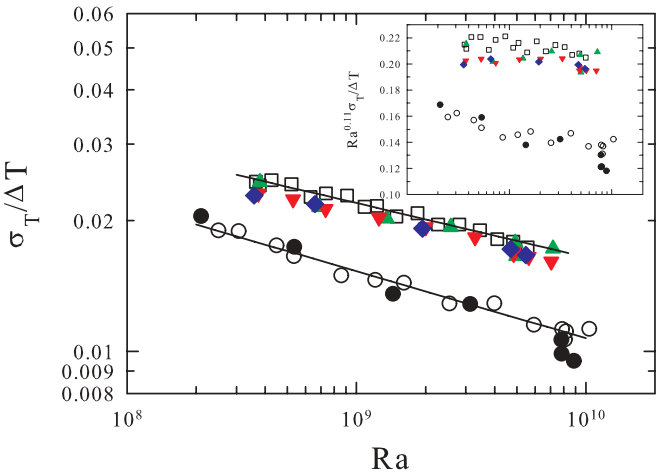

FIG. 13. (Color online) $\sigma_T/\Delta T$ measured near the sidewall as a function of Ra: (open circles) smooth cell, $c = 0$; (solid circles) smooth cell, $c = 120$; (open squares) rough cell, $c = 0$; (solid triangles) rough cell, $c = 120$; (solid inverted triangles) rough cell, $c = 150$; (solid diamonds) rough cell, $c = 180$. The solid lines represent power-law fits to the $c = 0$ case in the smooth and rough cells, respectively. (Inset) Compensated plots of the same data as in the main figure.

TABLE I. Fitted values of the power-law amplitude A and exponent β for the normalized temperature standard deviation $\sigma_T/\Delta T$ measured in both the smooth and rough cells and at the cell center and sidewall, respectively, with different polymer concentration c.

Cell	Quantity	c (ppm)	A	$\beta(\pm 0.01)$
Smooth	σ_T(center)/ΔT	0	0.06 ± 0.01	-0.10
	σ_T(center)/ΔT	120	0.06 ± 0.01	-0.10
	σ_T(side)/ΔT	0	0.37 ± 0.05	-0.15
	σ_T(side)/ΔT	120	0.9 ± 0.2	-0.20
Rough	σ_T(center)/ΔT	0	0.05 ± 0.01	-0.07
	σ_T(center)/ΔT	120–180	0.06 ± 0.01	-0.08
	σ_T(side)/ΔT	0	0.29 ± 0.03	-0.12
	σ_T(side)/ΔT	120–180	0.25 ± 0.03	-0.12

near the sidewall and none for the rough cell as far as we know. The one experimental result that we are aware of gives $\beta = -0.24 \pm 0.03$ [27], which differs somewhat from the present result for the $c = 0$ case. However, this discrepancy should be viewed in the light that the reported values of β (at cell center) usually differ markedly from each other and have large error bars. What is interesting is that, unlike in the cell center, here β does not seem to change much for the smooth and rough cells.

The statistical characteristics of local temperature fluctuations, as quantified by the measured probability density functions (PDFs), do not seem to change with the additions of polymers, nor do they show a sensitive dependence on whether the cell surface is smooth or rough. These are shown in Figs. 14 and 15 for the smooth and rough cells, respectively. It can be seen that the PDFs in the cell center exhibit symmetric exponential distributions. Near the sidewall, the measured PDFs exhibit skewed exponential distributions, which may be understood by the fact that near the sidewall the flow is usually dominated by either hot upward or cold downward flows. These results are consistent with previous studies in both smooth and rough cells without polymer additives [28,29].

C. Velocity and Reynolds number behavior

As discussed in Sec. II D, the speed of the large-scale circulation can be determined from the period of local temperature oscillations. Here we use data measured with a thermistor placed near the cell sidewall at midheight. In Figs. 16(a) and 16(b), we examine the measured LSC velocity U and the corresponding Reynolds number $\mathrm{Re} = UH/\nu(c)$ in the smooth cell. The results of best power-law fits $\mathrm{Re} = ARa^{\gamma}$ to these data are given in Table II and we see that the Ra scaling exponent is about 0.45. In the figure, for clarity, only fittings for the $c = 0$ case are shown (solid lines). These results show that within experimental uncertainties both the amplitude and the Ra scaling exponent of the LSC velocity remain essentially unchanged when polymers are added to the convecting fluid. For the Reynolds number Re, although the exponent does not seem to change with the addition of polymers (the difference between the exponents for U and for Re for the $c = 120$ ppm case shown in Table II is due to rounding off), the amplitude is clearly decreased (by about 13%) and this can be understood by the increased viscosity of the fluid. As shown in Figs. 17(a) and 17(b), the situation differents substantially in the rough cell.

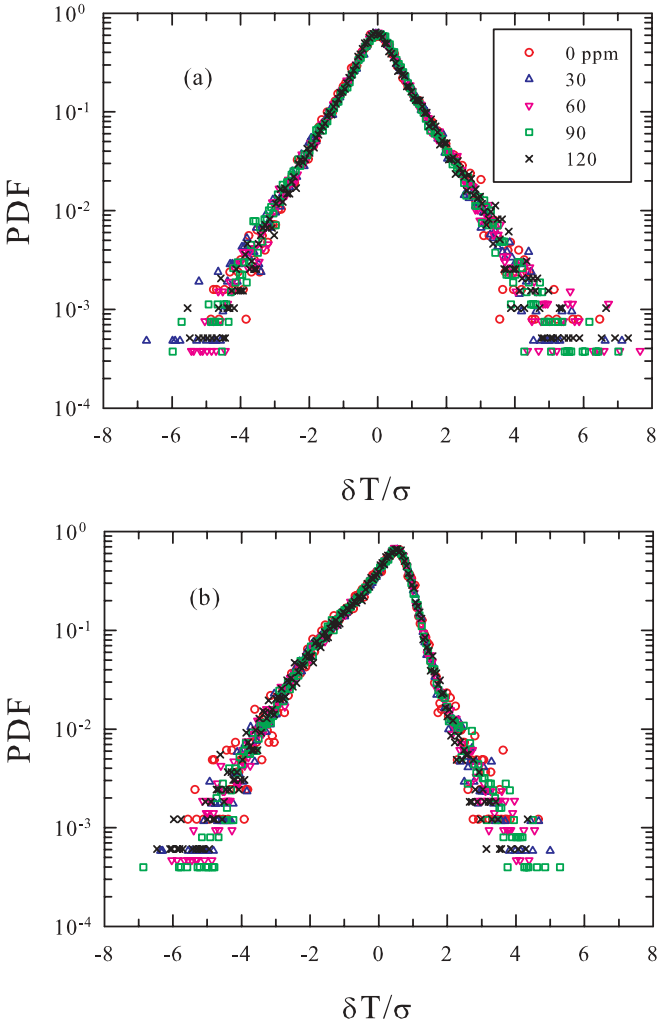

FIG. 14. (Color online) Temperature PDF from the smooth cell ($\mathrm{Ra} = 8 \times 10^9$) for various values of polymer concentrations: (a) measurements are made at the cell center and (b) near the sidewall. The symbols are the same as those in (a).

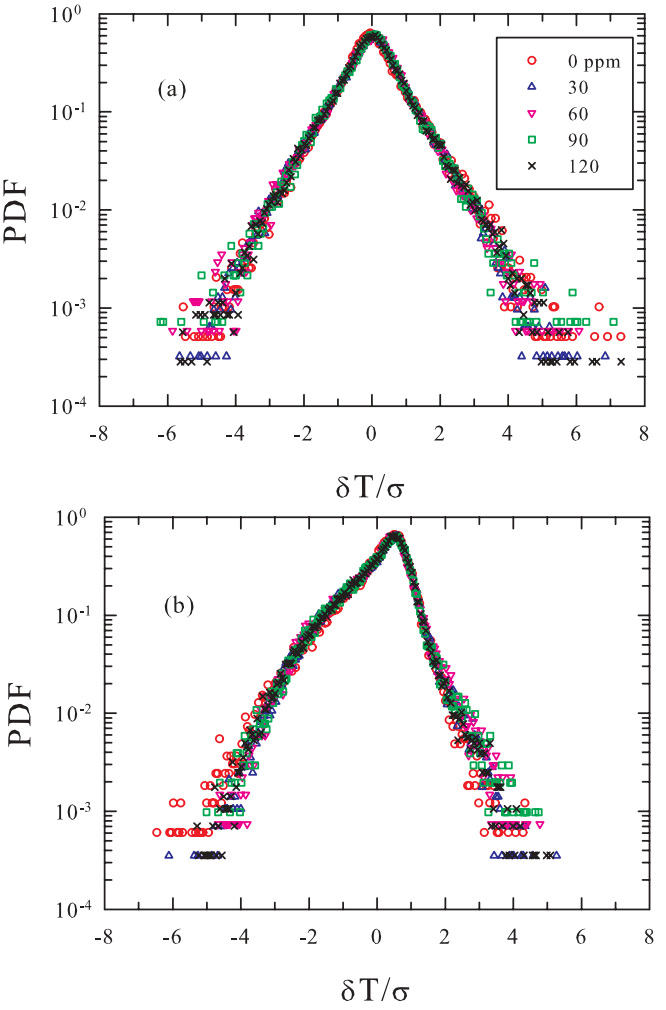

FIG. 15. (Color online) Temperature PDF from the rough cell ($\mathrm{Ra} = 5.4 \times 10^9$) for various values of polymer concentrations: (a) measurements are made at the cell center and (b) near the sidewall. The symbols are the same as those in (a).

First, the magnitude of the LSC velocity is increased when polymers are added (∼7% compared to the case of pure fluid). The best power-law fits in this case give similar exponents as in the smooth case and the fitting results are also listed in Table II. To further compare the smooth and rough cell results, we plot in Fig. 18(a) the velocity U reduced by $\mathrm{Ra}^{0.45}$ measured in both smooth and rough cells, with and without polymers. This compensated plot shows clearly that in the rough cell the LSC velocity is indeed increased in fluid with polymer additives as compared to that of the pure fluid, whereas in the smooth cell U remains essentially unchanged when polymers are added. Figure 18(b) shows compensated plots of Re vs Ra and it is seen that, due to the increased solution viscosity, in both smooth and rough cells the Reynolds number is decreased when polymers are added.

To better compare the amplitude of the LSC velocity U for different c, we fix the scaling exponent at 0.45 and then fit the data again with a power law. This gives $U = (8.94 \pm 0.03, 9.38 \pm 0.02, 9.61 \pm 0.07, 9.73 \pm 0.07) \times 10^{-7}\mathrm{Ra}^{0.45}$ (m/s), where the amplitudes in the brackets are for $c = 0$, 120, 150, and 180 ppm, respectively. These results show clearly that the amount of velocity enhancement increases with increasing polymer concentration within the parameter range of the experiment. To find the concentration dependence of U and Re, we plot in Fig. 19 the normalized $U(c)/U(0)$ and $\mathrm{Re}(c)/\mathrm{Re}(0)$ vs c for several values of Ra (note

TABLE II. Fitted values of the power-law amplitude A and exponents γ for the LSC velocity U and the Reynolds number Re in both the smooth and rough cells and with different polymer concentration c.

Cell	Quantity	c (ppm)	A	$\gamma(\pm 0.01)$
Smooth	U	0	$(6 \pm 1) \times 10^{-7}$	0.45
	U	120	$(6 \pm 2) \times 10^{-7}$	0.45
	Re	0	0.19 ± 0.03	0.45
	Re	120	0.16 ± 0.03	0.46
Rough	U	0	$(8.2 \pm 0.7) \times 10^{-7}$	0.45
	U	120–180	$(9 \pm 1) \times 10^{-7}$	0.45
	Re	0	0.25 ± 0.02	0.45
	Re	120–180	0.23 ± 0.03	0.45

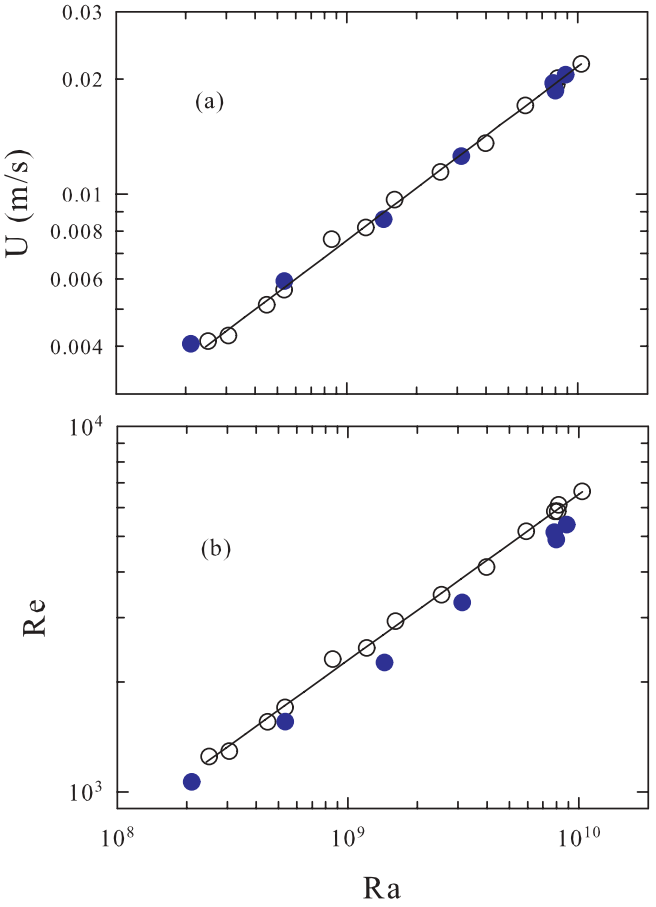

FIG. 16. (Color online) (a) LSC velocity U as a function of Ra measured in the smooth cell: (open circles) $c = 0$, (solid circles) $c = 120$. (b) $\mathrm{Re} = UL/\nu(c)$ as a function of Ra, with U corresponding to those in (a). The solid lines represent power-law fits to the $c = 0$ case.

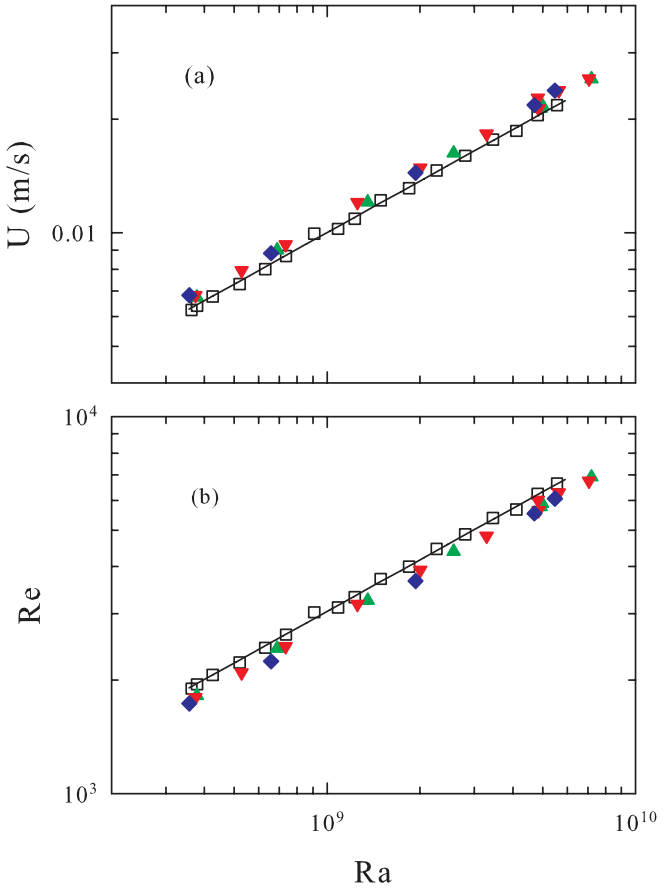

FIG. 17. (Color online) (a) LSC velocity U as a function of Ra measured in the rough cell: (open squares) $c = 0$, (solid triangles) $c = 120$, (solid inverted triangles) $c = 150$, and (solid diamonds) ($c = 180$). (b) $\mathrm{Re} = UL/\nu(c)$ as a function of Ra, with U corresponding to those in (a). The solid lines represent power-law fits to the $c = 0$ case.

that there is only one complete c scan at $\mathrm{Ra} = 5.4 \times 10^9$). The figure shows clearly the enhanced velocity at high polymer concentrations and it moreover shows that there is a threshold for the velocity enhancement, i.e., it occurs only for $c \geqslant 90$.

IV. DISCUSSIONS

While the exact mechanisms that lead to the reduction in the smooth cell and enhancement in the rough cell of heat transport by polymer additives remain unknown to us, we nevertheless attempt to provide a few scenarios that are unavoidably speculative in nature. The aim is not to provide some definitive explanations but to stimulate more works in this subject.

Before discussing the effect of polymers, for ease of discussion let us briefly recall some earlier results obtained in both smooth and rough cells in pure fluids. First, it is generally accepted that thermal plumes are formed from thermal boundary layers that are detached from the plates as a result of instability. It is also known that these plumes are the main carriers of heat transport. In fact, they play a dominant role in heat transport in turbulent RB convection [30,31]. With rough surfaces on the top and bottom plates, heat transport is greatly enhanced which may be understood as a result of enhanced plume emissions at the tip of the roughness elements (the pyrimand) [11,32,33]. This enhanced plume emission implies an increase in BL instability as the BLs are perturbed by the roughness elements. From previous studies over similar range of Ra and in the same geometry and aspect ratio, it has been found that the thermal BL thickness changed from 3 to 0.8 mm and the viscous BL thickness from 5 to 3 mm when Ra was increased from its lowest to highest values of the range spanned [34,35]. As already mentioned, the height of the roughness elements in the rough cell is $k = 8$ mm. Therefore, both the thermal and the viscous boundary layers are being perturbed strongly in the rough cell. It is obvious that the very different behaviors observed in the smooth and rough cells lie in the boundary layers.

In the smooth cell, it has been shown that the viscous boundary layer is laminar and can be described by the Prandtl-Blasius BL theory [36–40]. It has been argued that the reduction of Nu in the smooth cell may be attributed by the increased drag in the laminar boundary layers that result from the increased viscosity by polymer additives [5]. In fact, the increased drag in the boundary layers has two effects; it not only slows down the flow but also makes the BLs more stable and, therefore, emits fewer plumes. Certainly, more

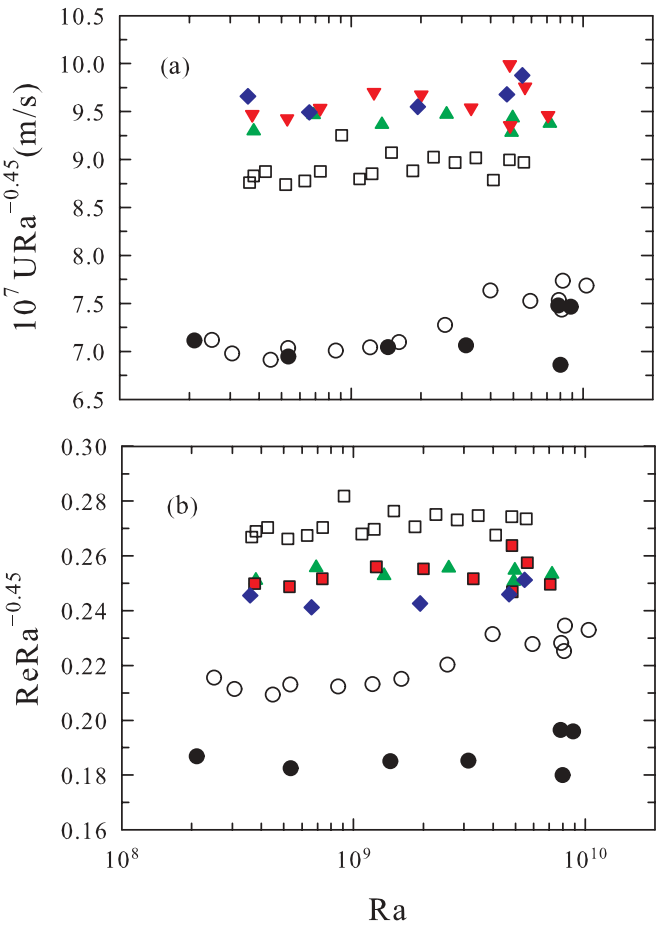

FIG. 18. (Color online) (a) LSC velocity U reduced by $Ra^{0.45}$ vs Ra. (Open squares) $c = 0$, rough cell; (solid triangles) $c = 120$, rough cell; (solid inverted triangles) $c = 150$, rough cell; (solid diamonds) $c = 180$, rough cell; (open circles) $c = 0$, smooth cell; and (solid circles) $c = 120$, smooth cell. (b) $ReRa^{-0.45}$ vs Ra. The symbols are the same as in (a).

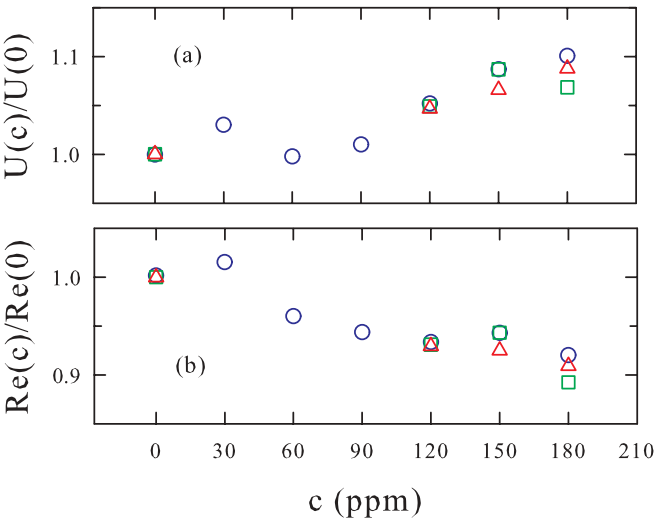

FIG. 19. (Color online) From the rough cell, (a) $U(c)/U(0)$ and (b) $Re(c)/Re(0)$ vs c for several values of $Ra = 8 \times 10^9$ (circles), 1.3×10^9 (squares), and 3.7×10^8 (triangles).

experimental evidence on the nature of BL modification is needed to substantiate this argument.

In the rough cell, it has been known that the surface roughness perturbs the BL and enhances heat transport (in the absence of polymers) [32,33]. Our recent study of heat transport in cells with both top and bottom plates being smooth ("both smooth"), one smooth and one rough ("half rough"), and both plates being rough ("both rough") have shown an increased Nu consistent with the system moving progressively from a more BL-dominated state to a more bulk-dominated state [9]. We also found that, under the Grossmann and Lohse model of decomposing energy dissipation into BL and bulk contributions [8], these results may be understood in terms of the flow state moving from a BL-dominated dissipation to a more bulk-dominated dissipation as the configuration is changed from "both smooth" to "half rough" to "both rough" [9]. When polymers are added to the flow, both the Nu and the large-scale circulation speed are observed to increase. These results suggest that the polymers are doing something to the turbulent bulk flow. That the polymer additives are affecting the bulk flow can be also seen from the measured local temperature fluctuations in the cell center shown in Fig. 10.

We note that almost all theoretical models of turbulent drag reduction by polymer additives require the deformation or stretching of polymer coils. In the present case, the shear rate generated by the turbulent flow would appear to be unable to induce stretching of the individual polymer chains. A previous light scattering study of PEO polymers in aqueous solutions has found that the polymers form clusters (or aggregates) with sizes much larger than the individual polymers [41]. Therefore, a possible scenario is that these clusters are sufficiently large and floppy that they are being stretched by the flow, rather than the individual polymers. Certainly more studies on the polymer conformations and polymer-flow interaction are needed to support this picture. Another scenario is proposed in Ref. [5] based on the direct numerical simulation (DNS) study of homogeneous (or bulk) turbulent RB convection. In that study it is reported that thermal plumes become more coherent when polymers are present. The argument here is that as plumes are known to be main heat carriers in turbulent RB convection [30,31], the increased plume coherence presumably enhances heat transport. In the present study, the measured rms values of the Nu (Fig. 9) and the local temperature (Fig. 10) also provide indirect evidence that support the enhanced plume coherence.

To see this, we first note that, unlike the DNS study that has no BLs, in the experiment with rough surfaces the BLs, although strongly perturbed, are not completely destroyed. This means that the measured quantities have contributions from both the BL and the bulk and the rough cell results have to be compared with the corresponding smooth cell results rather than with their own. For example, from Fig. 8 one sees that the rms value of Nu in the smooth cell decreases with increasing polymer concentration before leveling off for $c \geqslant 120$ ppm. In contrast, from Fig. 9 we see that σ_{Nu} in the rough cell is approximately the same for all concentrations. Similar behavior is also observed for the rms fluctuations of local temperature measured at cell center. The decreasing level of fluctuations of both the Nu and the local temperature with increasing polymer concentration in the smooth cell may be understood as a result of reduced plume emissions. With

fewer plumes, both the local and global fluctuations of the temperature field are reduced. In the rough cell, the added polymers would still make the BLs more stable and thus emitting less plumes. But now BLs are less dominant than the bulk. As the total level of fluctuations are now roughly constant with respect to polymer concentration, it suggests that temperature fluctuations in the bulk have to increase in order to compensate the decrease from the BLs. This increase is conceivably coming from an increase in the coherence of the plumes, as less coherent or more fragmented (well-mixed) plumes will result in a smoother temperature field. Again, direct local measurements of the properties of polymers and plumes are needed to support these scenarios.

When combining the velocity results with those for Nu and local temperature fluctuations from Sec. III B, we may qualitatively understand the observed Nu behavior as follows. We discuss the case for the smooth cell first. From Figs. 8 and 10(a) it is seen that both σ_{Nu} and $\sigma_T/\Delta T$ decrease with increasing polymer concentration c and then level off for $c \geqslant 120$ ppm, whereas the LSC velocity remains essentially unchanged with and without polymers. If we take the Nusselt number as the product of local temperature fluctuations and the velocity of the LSC, then this behavior corresponds to that of global Nu vs c as shown in Fig. 6. For the rough cell, both σ_{Nu} and $\sigma_T/\Delta T$ show no appreciable change over the range of polymer concentration, whereas the LSC velocity increased for about 7% for $c = 120$–180 ppm over that of pure liquid. When combined, this can produce an Nu enhancement. Indeed, even the magnitude of the increase in U roughly matches the increase of global Nu ($\sim$4%).

Finally, we wish to point out that the effect of polymer additives on the inertial-driven and thermally driven turbulence may not be the same. As shown by Cadot *et al.* [42] in a study using von Karman flows, turbulent drag reduction by polymers is essentially a boundary layer phenomenon and no reduction can be sustained in the bulk of the turbulent flow. On the other hand, inertial-driven and thermally driven turbulent flows need not have the same mechanisms for polymer-flow interactions, as thermal plumes are absent in the former case. Indeed, an enhanced heat transfer does not necessarily imply a drag reduction and, therefore, does not necessarily require the stretching of polymers.

V. SUMMARY AND CONCLUSIONS

We have presented an experimental study of turbulent thermal convection with polymer additives using convection cells with smooth and rough top and bottom plates, respectively. Heat transport, local temperature fluctuations, and velocity measurements were made. The study found both reduction and enhancement in the measured Nusselt number, depending on the boundary condition of the solid top and bottom conductive plates. We stress here that the main focus of the paper is to present experimental results and that the mechanisms of the heat transport reduction in the smooth cell and enhancement in the rough cell, as well as the nature of polymer-flow interaction, remain unknown at present. Our main findings are as follows.

For plates with smooth surfaces, a reduction of the Nu was observed. A new finding in the present study is that for polymer concentration $c \geqslant 120$ ppm, the decrease in Nu apparently levels off, suggesting a saturation of the underlying effect that is responsible for the Nu decrease. A possible reason for the Nu reduction may be related to the increased drag in the boundary layers. For plates with rough surfaces, an enhancement of Nu was observed.

Examinations of the fluctuations of the global Nu and of the local temperature found that, in the smooth cell, the standard deviations of Nu and local temperature in the cell center have similar dependence on polymer concentration as that of Nu itself, i.e., they all decrease with increasing c and level off for $c \geqslant 120$ ppm. In contrast, the fluctuations of both the global Nu and the local temperature in the rough cell are found to be essentially independent of polymer concentration.

From the velocity measurement, it is found that the velocity of the LSC in the smooth cell is essentially the same with and without polymers. In contrast, the measured LSC velocity in the rough cell is increased when polymers are added to the convecting fluid. Moreover, the magnitude of the velocity appears to increase with increasing polymer concentration. The Reynolds number of the LSC, on the other hand, is decreased when polymers are added in both the smooth and the rough cells, with the amount of decrease being larger for the smooth cell. This decrease may be understood by the increased viscosity of the polymer solution.

ACKNOWLEDGMENTS

We thank G. Ahlers for suggesting the use of Teflon-coated surfaces. We also thank X. Z. Zhao and S. D. Huang for their help with the experiment and T. S. Chan for making his data available to us. This work was supported by the Research Grants Council of Hong Kong SAR (No. CUHK404409).

[1] I. Procaccia, V. S. L'vov, and R. Benzi, Rev. Mod. Phys. **80**, 225 (2008).
[2] G. Ahlers, S. Grossmann, and D. Lohse, Rev. Mod. Phys. **81**, 503 (2009).
[3] D. Lohse and K.-Q. Xia, Annu. Rev. Fluid Mech. **42**, 335 (2010).
[4] G. Ahlers and A. Nikolaenko, Phys. Rev. Lett. **104**, 034503 (2010).
[5] R. Benzi, E. S. C. Ching, and E. De Angelis, Phys. Rev. Lett. **104**, 024502 (2010).
[6] G. Boffetta, F. De Lillo, and S. Musacchio, Phys. Rev. Lett. **104**, 034505 (2010).
[7] D. Lohse and F. Toschi, Phys. Rev. Lett. **90**, 034502 (2003).
[8] S. Grossmann and D. Lohse, Phys. Rev. Lett. **86**, 3316 (2001).
[9] P. Wei, R. Ni, T. S. Chan, and K.-Q. Xia (submitted for publication).
[10] S.-L. Lui and K.-Q. Xia, Phys. Rev. E **57**, 5494 (1998).
[11] X.-L. Qiu, K.-Q. Xia, and P. Tong, J. Turb **6**, 30 (2005).

[12] Y.-B. Du and P. Tong, J. Fluid Mech. **407**, 57 (2000).
[13] D. Viswanath, *Viscosity of Liquids: Theory, Estimation, Experiment, and Data* (Springer, Berlin, 2007).
[14] M. Rubinstein and R. H. Colby, *Polymer Physics* (Oxford University Press, Oxford, UK, 2003).
[15] D. Bonn and J. Meunier, Phys. Rev. Lett. **79**, 2662 (1997).
[16] J. S. Steinhart and S. R. Hart, Deep-Sea Res. Oceanogr. Abstr. **15**, 497 (1968).
[17] X.-D. Shang and K.-Q. Xia, Phys. Rev. E **64**, 065301 (2001).
[18] X.-L. Qiu and P. Tong, Phys. Rev. E **66**, 026308 (2002).
[19] X.-L. Qiu, X.-D. Shang, P. Tong, and K.-Q. Xia, Phys. Fluid **16**, 412 (2004).
[20] C. Sun, K.-Q. Xia, and P. Tong, Phys. Rev. E **72**, 026302 (2005).
[21] S.-Q. Zhou, C. Sun, and K.-Q. Xia, Phys. Rev. E **76**, 036301 (2007).
[22] H.-D. Xi, S.-Q. Zhou, Q. Zhou, T.-S. Chan, and K.-Q. Xia, Phys. Rev. Lett. **102**, 044503 (2009).
[23] C. Sun and K.-Q. Xia, Phys. Rev. E **72**, 067302 (2005).
[24] T.-S. Chan, M.Phil. thesis, The Chinese University of Hong Kong, 2008.
[25] K.-Q. Xia, S. Lam, and S.-Q. Zhou, Phys. Rev. Lett. **88**, 064501 (2002).
[26] Z. A. Daya and R. E. Ecke, Phys. Rev. E **66**, 045301 (2002).
[27] X.-D. Shang, P. Tong, and K.-Q. Xia, Phys. Rev. Lett. **100**, 244503 (2008).
[28] K.-Q. Xia and S.-L. Lui, Phys. Rev. Lett. **79**, 5006 (1997).
[29] Y.-B. Du and P. Tong, Phys. Rev. E **63**, 046303 (2001).
[30] X.-D. Shang, X.-L. Qiu, P. Tong, and K.-Q. Xia, Phys. Rev. Lett. **90**, 074501 (2003).
[31] X.-D. Shang, X.-L. Qiu, P. Tong, and K.-Q. Xia, Phys. Rev. E **70**, 026308 (2004).
[32] Y. Shen, P. Tong, and K.-Q. Xia, Phys. Rev. Lett. **76**, 908 (1996).
[33] Y.-B. Du and P. Tong, Phys. Rev. Lett. **81**, 987 (1998).
[34] Y.-B. Xin, K.-Q. Xia, and P. Tong, Phys. Rev. Lett. **77**, 1266 (1996).
[35] Y.-B. Xin and K.-Q. Xia, Phys. Rev. E **56**, 3010 (1997).
[36] C. Sun, Y.-H. Cheung, and K.-Q. Xia, J. Fluid Mech. **605**, 79 (2008).
[37] Q. Zhou and K.-Q. Xia, Phys. Rev. Lett. **104**, 104301 (2010).
[38] Q. Zhou, R. J. A. M. Stevens, K. Sugiyama, S. Grossmann, D. Lohse, and K.-Q. Xia, J. Fluid Mech. **664**, 297 (2010).
[39] Q. Zhou, K. Sugiyama, R. J. A. M. Stevens, S. Grossmann, D. Lohse, and K.-Q. Xia, Phys. Fluid **23**, 125104 (2011).
[40] R. J. A. M. Stevens, Q. Zhou, S. Grossmann, R. Verzicco, K.-Q. Xia, and D. Lohse, Phys. Rev. E **85**, 027301 (2012).
[41] A. M. Shetty and M. J. Solomon, Polymer **50**, 261 (2009).
[42] O. Cadot, D. Bonn, and S. Douady, Phys. Fluid **10**, 426 (1998).